

Original paper

Uranium–niobium-rich alteration products after “písekite”, an intimate mixture of Y, REE, Nb, Ta, Ti-oxide minerals from the Obrázek I pegmatite, Písek, Czech Republic

Radek ŠKODA^{1*}, Milan NOVÁK¹, Jaroslav CÍCHA²¹ Department of Geological Sciences, Masaryk University, Kotlářská 2, 611 37 Brno, Czech Republic; rskoda@sci.muni.cz² Prácheň Museum, Velké náměstí 114, 397 24 Písek, Czech Republic

* Corresponding author



An improperly described association, further called “písekite” aggregate, of fine-grained, mostly metamict U, Th-enriched Y, REE, Nb, Ta, Ti-oxide minerals from Obrázek I pegmatite, Písek, forms an intimate mixture of polycrase-(Y), samarskite-(Y) and fergusonite-(Y). It underwent a low-temperature hydrothermal alteration the products of which are depleted in Y and REE > U and significantly enriched in Si, As and P. Two distinct assemblages of secondary phases were recognized to be associated with “písekite” aggregate, namely (i) that developed within the central parts of the aggregate and (ii) pocket assemblage in albite adjacent to it. Both assemblages are dominated by Fe-rich smectite. “Písekite” aggregate is intensively replaced by U, Nb, Ti, Fe, As, P-rich phases of variable chemical composition: phase A (Nb > Ti > Fe > U > As) from the first assemblage, as well as phases B (U ~ Nb > Ti > As > P > Fe) and C (U > Nb > As > Fe > Ti) from the second assemblage. Associated pharmacosiderite and kahlerite/metakahlerite as well as Fe-rich smectite indicate a low temperature of the alteration processes (less than 150–200 °C). Whereas the “písekite” aggregate was the likely source of U, Nb and Ti, arsenopyrite of the host pegmatite yielded As with Fe. The textural features show that the Fe-rich smectite replacement by the U, Nb-rich phases A, B and C took place on a micrometer scale, and these highly heterogeneous U, Nb-rich phases likely represent a mixture of nanoscale, possibly amorphous hydrated oxides, phosphates–arsenates as well as silicates of U, Fe and Ca.

Keywords: uranium, polycrase-(Y), samarskite-(Y), fergusonite-(Y), kahlerite, smectite

Received: 4 May 2011; **accepted:** 21 September 2011; **handling editor:** J. Plášil

1. Introduction

Primary Y, REE, Nb, Ta, Ti-oxide minerals from granitic pegmatites enriched in U and Th (of the aeschynite, euxenite, samarskite, fergusonite and pyrochlore groups) commonly undergo intense hydrothermal alterations enhanced also by their tendency to become metamict with time (Ewing 1975). Metamictization, i.e. the transition from a crystalline to an amorphous state, is accompanied by major changes in chemical and physical properties. Amorphous minerals are usually hydrated and amorphization generally decreases their chemical durability. Altered metamict Y, REE, Nb, Ta, Ti-oxide minerals commonly show enrichment in Si, Al and Ca, whereas Y and REE, in particular, are released from the system (e.g. Nasraoui and Bilal 2000; Ercit 2005; Geisler et al. 2005; Ruschel et al. 2010). Uranium and thorium are also selectively removed, leaving behind B-site cations – Nb, Ta and Ti (Ewing 1975; Geisler et al. 2005). These alteration products also occur in the metamict state and they are generally assigned to the pyrochlore-group minerals based solely on the chemical composition (e.g., Ercit 2005).

“Písekite” (Krejčí 1923) is an improperly described fine-grained mixture of metamict Y, REE, Nb, Ta, Ti-oxide minerals close to samarskite (Bouška and Johan 1972) from granitic pegmatites of the Písek region. It is typically strongly altered and rare relics of primary phases revealed that the “písekite” represents an intimate mixture of several primary Y, REE, Nb, Ta, Ti-oxide minerals compositionally related to polycrase-(Y), samarskite-(Y) and fergusonite-(Y) (Škoda et al. 2010). They are commonly intimately intergrown with columbite-(Fe) and zircon (Škoda et al. 2010). The list of secondary minerals replacing “písekite” includes scheelite, ixiolite, rutile, zirconolite, galena and REE,U-rich pyrochlore-group minerals (Breiter et al. 2010; Škoda et al. 2010).

In the studied assemblages, secondary minerals either directly pseudomorph altered “písekite” aggregate or they are developed in small pockets in primary albite adjacent to the “písekite” aggregate. Moreover, these assemblages contain several phases hitherto unknown from the “písekite” aggregates. Textural relations and chemical composition of the individual secondary phases are given in the current text along with a discussion regarding their possible source and mobility of the individual elements.

2. Methods

Electron microprobe analyses (EMPA) of carbon-coated polished sections were obtained by a Cameca SX 100 instrument (Joint Laboratory of Electron Microscopy and Microanalysis, Institute of Geological Sciences, Masaryk University, and Czech Geological Survey, Brno) using the wavelength-dispersion mode. The following analytical conditions were applied: accelerating voltage of 15 kV, beam diameter of 2–5 μm , beam current of 20 nA, counting times of 20 s for Nb, Ta, Ti, Ca, Y and 30–60 s for the other elements. The standards and lines used included: Ti (K_{α}) – TiO; Nb (L_{α}), Fe (K_{α}) – columbite-(Fe) (Ivigtut); Ta (M_{α}) – CrTa_2O_6 ; Mn (K_{α}) – Mn_2SiO_4 ; Ca (K_{α}), W (M_{β}) – CaWO_4 ; Na (K_{α}) – albite (Amelia mine); P (K_{α}) – $\text{Ca}_5(\text{PO}_4)_3\text{F}$; K, Al, Si (K_{α}) – sanidine (Eifel); Mg (K_{α}) – Mg_2SiO_4 ; As (L_{α}) – lammerite (Guanaco), Y (L_{α}) – YAG; Sn (L_{α}) – SnO_2 ; U (M_{β}) – U; Th (M_{α}) – ThO_2 ; Sc (K_{α}) – ScVO_4 ; Pb (M_{α}) – vanadinite (Mibladen); Zr (L_{α}) – ZrSiO_4 ; La, Ce, Er, Yb (L_{α}); Pr, Nd, Sm, Gd, Dy, (L_{β}) – La–Dy orthophosphates; Er – $\text{Y}_{0.5}\text{Er}_{0.5}\text{AlO}_3$; Yb – YbAlO_3 . Europium, Tb, Ho, Tm and Lu were not measured. Data were reduced using the PAP routine (Pouchou and Pichoir 1985). Relative errors are estimated to be < 1 % at the >10 wt. % level, 10–20 % at the ~ 1 wt. % level and >20 % at the <0.5 wt. % level. The smectite/chlorite analyses were collected using 15 kV of accelerating voltage, 10 nA of beam current and 5 μm of beam size. The kahlerite/metakahlerite was analyzed at 15 kV and 2 nA by beam 5 μm in diameter. The standards were similar to those described above.

The X-ray maps were acquired in continuous stage-move mode using WDS spectrometers, 15 kV of accelerating voltage, 60 nA of beam current, >1 μm beam size, 0.5 μm step and dwell time of 100 ms per pixel.

3. Occurrence

Variscan pegmatites from the Písek region cut migmatized gneisses and amphibole–biotite syenites (durbachites) of the Mehelník Massif, Moldanubian Zone (Novák et al. 1998; Breiter et al. 2010). Beryl pegmatites vary from less evolved and small dikes with common tourmaline and rare beryl to large, textually highly differentiated and geochemically more fractionated pegmatite dikes, up to 25 m thick, with common tourmaline, beryl, and numerous accessory minerals (e.g., fluorapatite, niobian rutile, ilmenite, columbite–tantalite, “písekite”, monazite-(Ce), xenotime-(Y), zircon, cordierite–sekaninaite, almandine–spessartine, pyrite, and arsenopyrite). Zoned pegmatites typically show complexly zoned internal structure with a border granitic unit (Kfs + Qtz + Pl + Bt), a graphic unit (Kfs + Qtz \pm Bt), blocky K-feldspar and large quartz core.

In highly evolved dikes common albite unit (Ab + Qtz \pm tourmaline, rare muscovite) is developed between quartz core and blocky K-feldspar and it contains majority of accessory minerals. The latest primary unit is represented by thin aplitic veins (1–5 cm thick) cutting the remaining textural/paragenetic units (Čech 1985). Beryl pegmatites from the Písek area belong to beryl–columbite subtype of the rare-element class (Černý and Ercit 2005).

The pegmatite from Obrázek I quarry (GPS 49°18'36.541"N, 14°11'40.068"E) is one the most evolved and texturally differentiated pegmatite dikes in the Písek region and involves all textural/paragenetic units given above. Minerals from this locality were examined in several papers (e.g., “písekite” – Krejčí 1923, Bouška and Johan 1972; tourmaline – Povondra 1981; beryl – Sejkora et al. 1998; niobian rutile – Černý et al. 2007). However, internal structure and petrography of the individual units as well as crystal chemistry most of the minerals remain poorly known (Čech 1985; Breiter et al. 2010).

4. Results

4.1. “Písekite” aggregate and its alteration products

“Písekite” was found at several localities of more fractionated pegmatites in the Písek area. It forms elongated grains commonly arranged to radial aggregates, up to 2 cm long (Fig. 1). The color of “písekite” aggregates varies from brownish–black through greenish to yellow, depending on the degree and style of hydrothermal alteration. Its aggregates are enclosed in albite, K-feldspar, tourmaline and, rather rarely, in beryl. Relics of primary polycrase-(Y), samarskite-(Y) and fergusonite-(Y), commonly ~10–500 μm in size, were sporadically found in the altered mass (Fig. 2).

The polycrase-(Y) and samarskite-(Y) volumetrically dominate over the fergusonite-(Y) relics in the “písekite” aggregates examined in this study. The alteration of aggregate propagates from rim inwards and along fractures; effects of progressive alteration were observed in BSE images (Fig. 2). Chemical compositions of the polycrase-(Y) and samarskite-(Y) relics also show slight deviation from the ideal stoichiometry whereas chemical compositions of altered and the least altered parts differ significantly (Tab. 1). The altered areas are slightly enriched in Si and strongly depleted in Y + REE relative to their precursors. The enrichment in Si (up to 7.1 wt. % SiO_2), As (up to 8.2 wt. % As_2O_3) and P (up to 5.9 wt. % P_2O_5), slight depletion in U and negligible content of Y+REE are typical of the most altered zones. The altered zone appears to be enriched in Nb, Ti, Ta and Th relative to its



Fig. 1 The radial aggregate of “písekite” associated with schorl and monazite-(Ce) in albite. U Nového rybníka quarry, Písek area.

precursors. The EMPA totals of altered areas vary in the range of 88–96 wt. % of oxides (Tab. 1).

Two texturally and compositionally distinct assemblages of secondary U,Nb-rich minerals were recognized in the “písekite” aggregates. (i) Within the “písekite” aggregate occur small ($\sim 200 \mu\text{m}$) irregular aggregates of

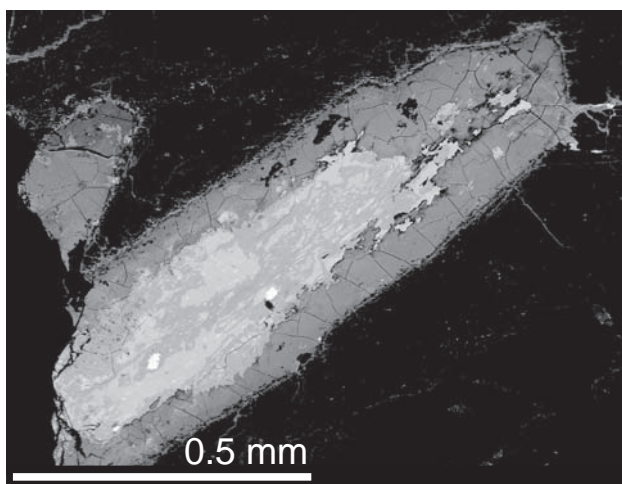


Fig. 2 Typical BSE image of “písekite” aggregate. Rare relics of intergrown primary polycrase-(Y), samarskite-(Y) and fergusonite-(Y) in central part are enclosed in weakly to moderately altered counterparts and surrounded by strongly altered rim.

randomly oriented flakes of Fe-rich smectite, $\sim 20 \mu\text{m}$ in size (Fig. 3a). They are interstitial among early replacement products of the “písekite” alteration. Chamosite, which is present in relics in the next assemblage and was the likely precursor to the Fe-rich smectite, was not found. (ii) Small pocket in primary albite, about several mm^3 in volume, was observed adjacent to an elongated “písekite” aggregate (Fig. 3b). The pocket is almost completely filled by a mixture of chamosite and a clay mineral (Fe-rich member of the smectite group) as randomly oriented flakes, $\sim 50\text{--}150 \mu\text{m}$ in size. Chamosite commonly forms internal parts of flakes and it is compositionally transitional to more common Fe-rich smectite. Its flakes are locally folded and deformed (Fig. 3b–c). The pocket is filled, along with dominant chamosite/smectite, by several other minerals: xenotime-(Y) \sim columbite-(Fe) $>$ zircon \sim fluorapatite \sim pharmacosiderite $>$ monazite-(Nd) (Fig. 3b–c). Columbite-(Fe) is evidently concentrated to the contact with “písekite” pseudomorph and its elongated euhedral crystals, up to $\sim 150 \mu\text{m}$ long, are generally parallel to the contact with “písekite” (Fig. 3b). Xenotime-(Y) forms euhedral grains, $\sim 100 \mu\text{m}$ in diameter, commonly located in the centre of the pocket (Fig. 3b). It is closely associated with euhedral crystals of zircon, up to $30 \mu\text{m}$ in diameter (Fig. 3b). Textural relations and morphology of the grains rather indicate that these minerals probably crystallized as early phases in the pocket, preceding the chamosite. Fluorapatite and pharmacosiderite are always closely associated as irregular intergrowths, $\sim 50 \mu\text{m}$ in size (Fig. 3c) concentrated in the parts of the pocket more distant from the “písekite” aggregate. Pharmacosiderite obviously replaces fluorapatite grains.

4.2. Secondary U, Nb-rich phases

4.2.1. Secondary assemblage developed within central parts of the “písekite” aggregates

In this assemblage, volumetrically dominant Fe-rich smectite is intensively replaced by Nb,Si,Ti,Fe,U,Ca-rich **phase A** of highly variable composition (Tab. 1). It is dominated by Nb_2O_5 (49.5–57.7 wt. %), SiO_2 (6.3–11.8 wt. %), TiO_2 (6.4–7.7 wt. %), Fe_2O_3 (4.1–5.9 wt. %), UO_3 (1.3–4.0 wt. %) and CaO (2.3–2.9 wt. %) prevailing over As_2O_5 ($< \sim 1$ wt. %). Further oxides are present in the concentrations ≤ 1 wt. %; e.g., ~ 0.3 wt.% ThO_2 (Tab. 1), whereas REE were below the detection limit of the EMPA. The sum of the oxides is *c.* 98 wt. %. X-ray elemental maps and chemical analyses revealed strong zoning of this micaceous aggregate (Fig. 4, 5a). The border zone along the contact with the highly altered “písekite” aggregate is preferentially enriched in Si

Tab. 1 Representative analyses of minerals making up the “pisckite” aggregates (wt. %)

Nr.	polycrase-(Y) samarskite-(Y) fergusonite-(Y)		altered “pisckite”							U-rich phase A							partial replacement of smectite by phase B				phase B	phase C	kahlertite†					
	8	9	1	2	3	4	5	6	7	8	9	10	11	12	13	14	15	16	17	18	19	20	21	22	23	24	25	
WO ₃	0.67	9.91	1.93	0.17	0.39	0.55	0.13	0.14	0.70	0.45	0.33	0.60	nd															
P ₂ O ₅	0.00	0.00	0.00	5.94	0.31	0.94	0.40	0.42	5.63	8.70	8.80	2.96	3.25															
As ₂ O ₃	0.00	0.00	0.00	8.18	0.73	3.63	0.21	0.51	3.93	8.90	9.59	6.68	17.54															
Nb ₂ O ₅	26.91	33.45	42.17	23.96	57.91	35.65	8.75	0.93	10.86	11.00	18.65	23.86	nd															
Ta ₂ O ₅	9.55	10.41	6.30	8.78	0.56	0.00	0.62	0.25	0.07	0.00	0.00	0.38	nd															
SiO ₂	0.01	0.00	0.00	4.63	7.16	3.35	41.26	42.49	19.92	6.65	1.74	1.14	0.28															
TiO ₂	18.73	1.60	0.46	12.73	7.09	4.11	2.42	0.49	9.10	12.45	12.24	4.79	nd															
UO ₂	6.88	9.41	1.15	10.76	2.05	22.96	0.53	0.25	13.06	22.73	22.90	39.73	60.81															
ThO ₂	1.42	2.39	0.40	2.14	0.21	0.10	0.12	0.00	0.01	0.03	0.00	0.12	nd															
Sc ₂ O ₃	0.33	1.71	0.62	0.63	3.61	1.89	16.35	28.84	7.92	3.66	1.62	0.62	0.14															
Y ₂ O ₃	14.21	9.16	25.99	0.00	0.30	0.23	0.00	0.03	0.07	0.15	0.28	0.10	nd															
Nd ₂ O ₃	0.34	0.53	0.89	0.18	0.11	0.11	0.00	0.00	0.07	0.00	0.00	0.05	nd															
Sm ₂ O ₃	0.83	0.74	1.19	0.10	0.05	0.09	0.00	0.00	0.00	0.06	0.00	0.11	nd															
Gd ₂ O ₃	2.18	1.57	3.36	0.09	0.03	0.06	0.00	0.00	0.00	0.08	0.10	0.04	nd															
Dy ₂ O ₃	2.57	1.88	4.38	0.00	0.07	0.09	0.00	0.00	0.00	0.09	0.16	0.30	nd															
Er ₂ O ₃	1.54	1.11	3.24	0.00	0.69	0.21	1.24	0.10	0.26	0.09	0.00	0.10	0.10															
Yb ₂ O ₃	1.89	1.30	4.17	3.45	2.85	2.02	0.84	0.53	2.73	4.13	4.70	2.88	0.25															
CaO	3.03	1.09	0.65	0.07	0.07	0.05	0.03	0.03	0.04	0.02	0.11	0.04	nd															
MnO	0.73	1.26	0.01	6.71	5.05	2.71	8.67	10.69	11.30	7.14	4.74	5.33	4.03															
FeO	1.69	6.09	0.00	1.37	0.35	0.45	0.08	0.00	0.49	1.05	2.22	1.23	0.16															
PbO	0.46	0.62	0.39	0.13	0.09	0.06	0.05	0.05	0.13	0.23	0.11	0.09	nd															
Total	93.97	94.23	97.30	98.90	91.03	82.12	86.10	90.44	93.00	95.25	96.58	101.47	86.56															

Analyses numbered in the header of the table are plotted in Figs 5a, d and 6.

Note that smectite* is associated with phase A and smectite** with phase B.

nd – not detected, † – average from 3 analyses.

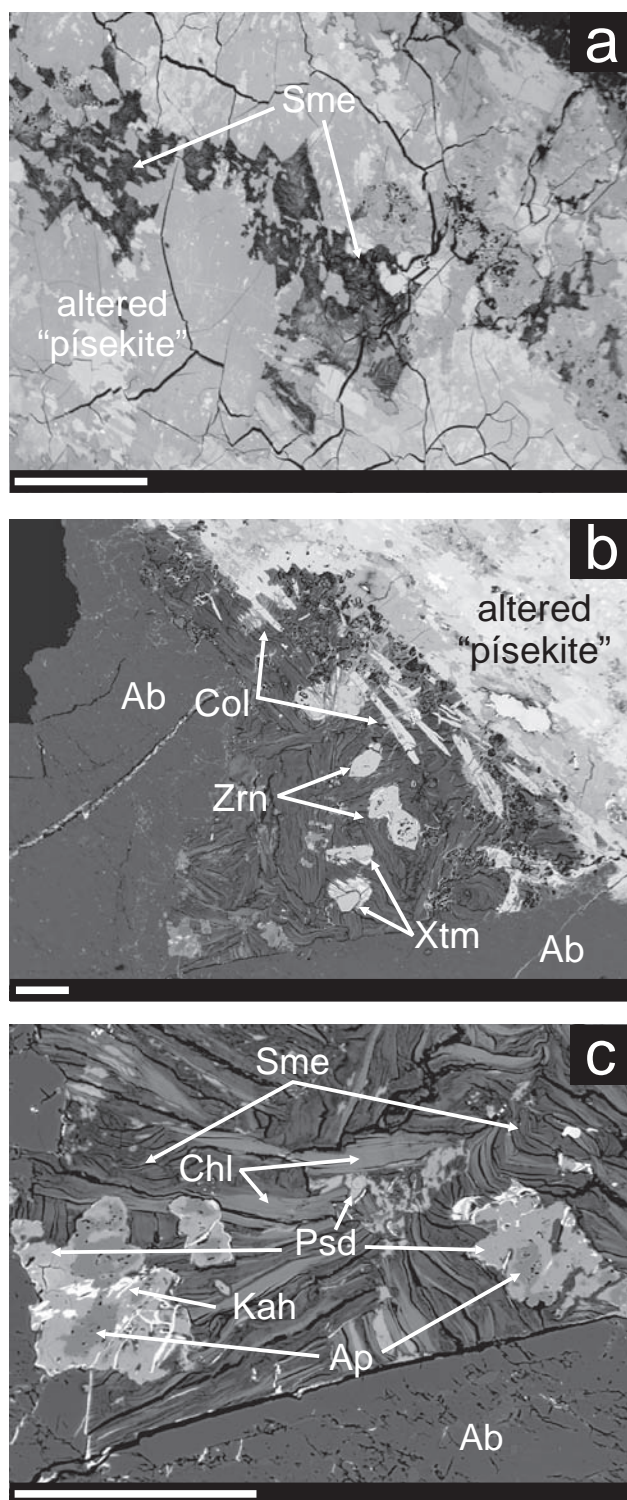


Fig. 3 Back-scattered electron (BSE) images of the typical “pisekite”-related assemblages. **a** – “Pisekite” aggregate; **b–c** Albite pocket. Mineral names abbreviations: albite (Ab), fluorapatite (Ap), zircon (Zrn), chamosite (Chl), columbite-(Fe) (Col), kahlerite/metakahlerite (Kah), pharmacosiderite (Psd), smectite-group mineral (Sme), xenotime-(Y) (Xtm). The scale bar is 100 μm in all figures.

and Al (smectite phase), whereas the central parts are depleted in Si and Al and enriched in Nb, Ti, Ca and Y. Uranium shows local enrichments (up to 23.0 wt. % UO_3) in the central parts (Fig. 4, 5a, Tab. 1).

4.2.2. Secondary U, Nb, Ti, Fe, As, P-phases in the albite pocket

The smectite flakes in the pocket are locally intensively replaced by U,Nb,Ti,Fe,As,P-phases of variable chemical composition. This replacement propagates along the cleavage and is spatially associated with aggregates of “pisekite” and crystals of columbite-(Fe) (Fig. 5b–c) or xenotime-(Y) (Fig. 5d). The replacement, spatially associated to “pisekite” and columbite-(Fe), is the most advanced along the contact with these phases, generally decreasing in intensity farther away. The spot (3 μm in diameter) electron-microprobe analyses differ significantly, showing a continuous variation from smectite to the **phase B** of the complex composition (Tab. 1): UO_3 (22.9 wt. %), Nb_2O_5 (18.7 wt. %), TiO_2 (12.2 wt. %), As_2O_5 (9.6 wt. %), P_2O_5 (8.8 wt. %), Fe_2O_3 (5.2 wt. %) and CaO (4.7 wt. %). The Th and Ta contents were below the detection limit of EMPA. The sum of the oxides is ~ 94 wt. %. Replacement of Fe-rich smectite spatially associated to xenotime-(Y) crystals, which are located farther from the “pisekite” aggregate, produced very similar textures (Fig. 5d) but the chemical composition differs, especially by higher contents of Nb and U. The most enriched and rather homogeneous **phase C** contains (see Tab. 1): UO_3 (39.7 wt. %), Nb_2O_5 (23.9 wt. %), As_2O_5 (6.7 wt. %), Fe_2O_3 (5.8 wt. %), TiO_2 (4.8 wt. %). The sum of the oxides is ~ 99 wt. %.

Further uraniferous phase found in this pocket forms aggregates, up to 50 μm in size, with sharp contact to chlorite/smectite. These aggregates frequently enclose relics of replaced fluorapatite (Fig. 5c) or occur in association with pharmacosiderite–fluorapatite intergrowths (Fig. 5d). The chemical composition of these aggregates is close to **kahlerite** or **metakahlerite** (average of 3 spot analyses): UO_3 (60.8 wt. %), As_2O_5 (17.5 wt. %), FeO (4.03 wt. %), P_2O_5 (3.25 wt. %) and CaO (0.3 wt. %). Other elements such as Mg, Na, Al and K are also present at levels below 0.25 wt. % of their respective oxides. The formula recalculation based on 2 cations in the tetrahedral site yields $\text{U}/(\text{As} + \text{P})$ close to 2:2, and occupation of the interlayer position ~ 0.65 *apfu*.

5. Discussion

Uranium-rich secondary phases forming at the expense of complex Nb,Ta,Ti,W-oxide minerals are rather rare in granitic pegmatites (e.g., Novák et al. 2008). At the

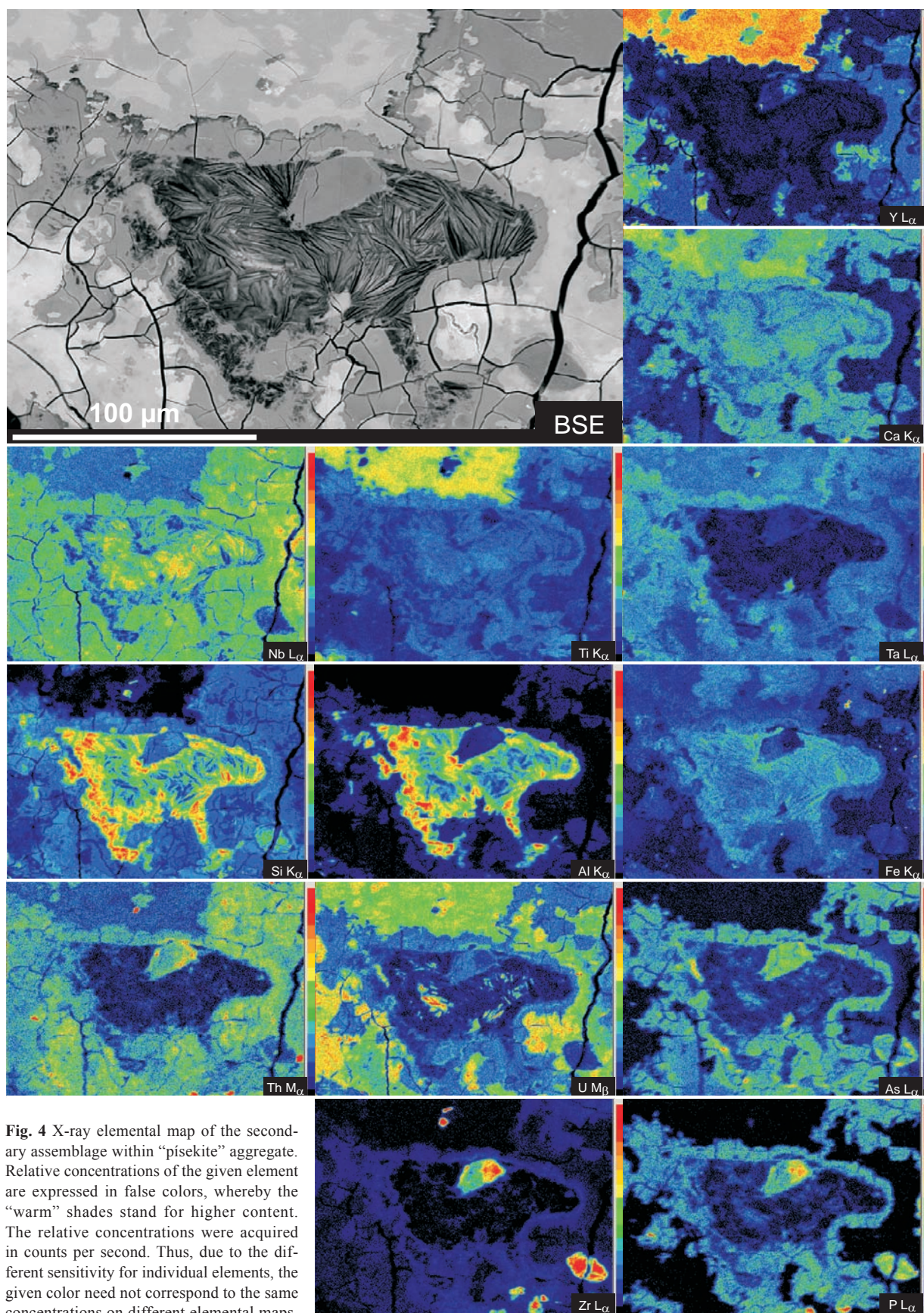


Fig. 4 X-ray elemental map of the secondary assemblage within "pisekrite" aggregate. Relative concentrations of the given element are expressed in false colors, whereby the "warm" shades stand for higher content. The relative concentrations were acquired in counts per second. Thus, due to the different sensitivity for individual elements, the given color need not correspond to the same concentrations on different elemental maps.

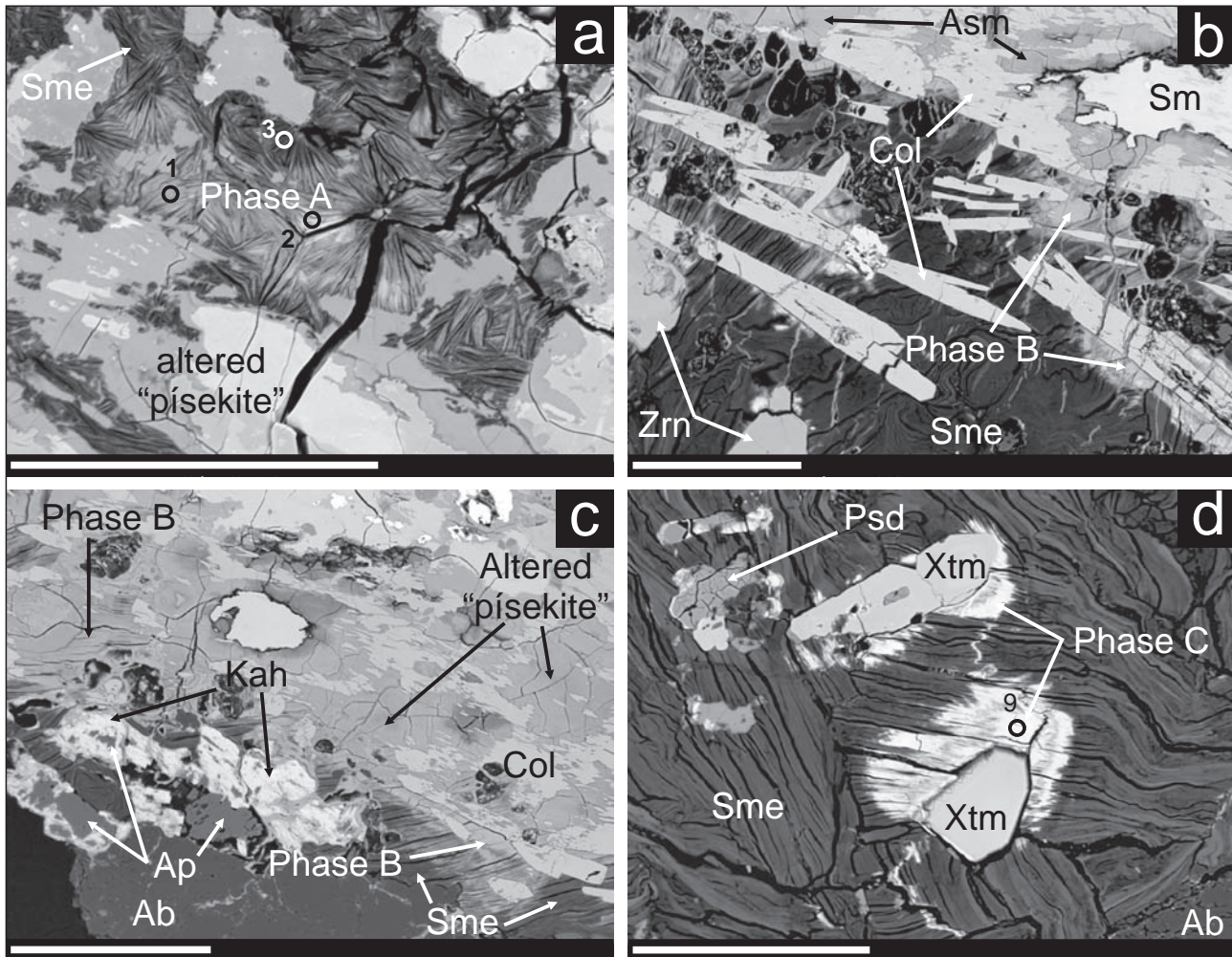


Fig. 5 Back-scattered electron (BSE) images of the phases A, B and C from the assemblages within the “písekite” aggregate (a) and from the albite pocket (b–d). The abbreviations of mineral names as in Fig. 3 except for altered samarskite (Asm) and samarskite-(Y) (Sm). The scale bar is 100 μm in all figures.

studied locality near Písek, we were able to distinguish three U, Nb-rich secondary phases in two mineral assemblages (Figs 3–5). All are evidently enriched in U, Nb, Ti, As, Fe relative to the original “písekite” aggregates but the compositions vary greatly. The phase A from the first assemblage (i), i.e. occurring within the “písekite” aggregate, shows $\text{Nb} > \text{Ti} > \text{Fe} > \text{U} > \text{As}$, whereas the phase B close to the “písekite” aggregate has $\text{U} \sim \text{Nb} > \text{Ti} > \text{As} > \text{P} > \text{Fe}$ and the phase C close to xenotime-(Y) grains exhibits $\text{U} > \text{Nb} > \text{As} > \text{Fe} > \text{Ti}$. Both latter phases come from the albite pocket assemblage (ii). Disregarding the contents of Ta and Th, the chemical composition of strongly altered “písekite” is very similar to the phase B, which occurs adjacent to the “písekite” aggregates (Tab. 1, Fig. 6). Hence, “písekite” aggregate was most probably the source of Nb, Ti and U, whereas the chlorite/smectite minerals provided Fe and Si. High As contents in some secondary minerals (pharmacosiderite, kahlerite/metakahlerite) and in altered zones of “písekite”

aggregate together with the absence of As in primary minerals (samarskite-(Y), polycrase-(Y), monazite-(Ce, Nd), fluorapatite) imply a participation of late fluids released during the arsenopyrite decomposition. It is a common accessory mineral in the Obrázek I pegmatite but occurs far from the “písekite” aggregates. In such likely acidic environment, apatite becomes unstable (e.g., Morton and Hallsworth 1999) and its dissolution may have released P present in alteration products but absent in the “písekite” aggregate itself (Tab. 1). However, altered feldspars also may be a source of P (e.g., London et al. 1990). Pharmacosiderite, a typical low-T alteration product of arsenopyrite (Drahota and Filippi 2009) as well as a smectite mineral (Dekov et al. 2008) provide an evidence that the hydrothermal alteration process was low-T ($< \sim 150\text{--}200\text{ }^\circ\text{C}$).

Given the limits of the analytical technique used in this study (EMPA), we cannot explicitly decide whether the examined phases A, B and C are individual miner-

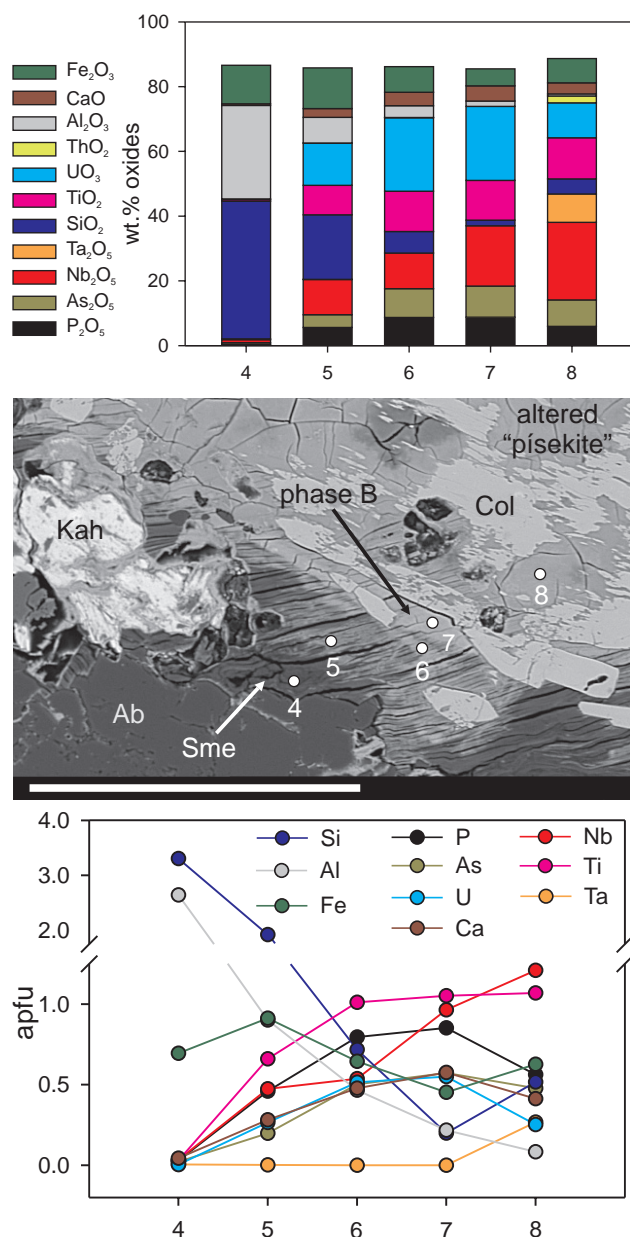


Fig. 6 Chemical composition of smectite, phase B and their transitional phases expressed in wt.% oxides (upper plot) and atoms per formula unit (apfu) in the lower plot. The mineral formulae were calculated by normalization to 12 anions, whereas Fe was considered as exclusively trivalent. The locations of analysed spots 4–8 are marked in the BSE image (center); the scale bar is 100 μm . The analyses are presented in Tab. 1; 4 – Fe-rich smectite, 5–6 – transitional phases, 7 – phase A, 8 – altered “písekite”.

als or mixtures of several phases. However, their quite complex chemical compositions suggest rather a mixture of nanoscale, possibly amorphous hydrated oxides, phosphates–arsenates and silicates of U, Fe and Ca. In addition, the recalculation of the mineral formula on the basis of oxygen atoms did not provide any reasonable elemental ratios. Transitional chemical composition be-

tween these phases and Fe-rich smectite (Tab. 1, Fig. 6) probably represents only partial replacement of smectite by newly-formed phases in analytical volume of EMPA (few μm^3). Despite the fact that they occur in various parageneses, the A, B and C phases replaced exclusively a smectite mineral. Hence smectite seems an appropriate precursor for low-T replacement at acidic conditions.

Kahlerite/metakahlerite is the only secondary U-rich phase that is close in composition to a recognized mineral. It differs from the other U,Nb-rich phases by the absence of Nb and Ti and, moreover, the textural and textural relations (Figs 3c, 4c), which indicate that it replaced early-formed fluorapatite and pharmacosiderite. The contacts with chlorite/smectite minerals are sharp with no indication of replacement. Hence, its origin seems different from the phases A, B and C, which evidently replaced chlorite/smectite aggregates.

The alteration of metamict “písekite” aggregates (polycrase-(Y) and samarskite-(Y) in the examined samples) led to a loss of Y + REE, and concomitant increase in Ca, Si, As, P and water contents in newly-formed secondary minerals (Tab. 1, Fig. 6). Release of Y + REE and their further absence in secondary phases suggests very high mobility of such elements at the given conditions. The chemical analyses also indicate that U and Th have a tendency to be incorporated into the altered (hydrated, Si, As, P, Ca, Fe-rich) parts of “písekite” aggregate. The additional dissolution of these altered parts led to a release of U, which precipitated in a form of iron uranyl arsenate (kahlerite/metakahlerite) or secondary U, Nb-rich phases A, B and C. Absence of secondary Th-bearing phases, very low Th contents in A, B, C phases, and decreasing U/(U + Th) ratio from the least to the most altered parts of “písekite” aggregate indicate evidently lower mobility of Th than U, probably due to the oxidation of U⁴⁺ to more mobile U⁶⁺.

The elucidation of alteration mechanisms producing U, Nb-rich phases is complicated by the very probable amorphous nature of the newly-formed phases and their small size. However, laboratory experiments and textural relations indicate that the dissolution and precipitation model (Pöml et al. 2007) operated. Similar compositional changes such as hydration, release of Y + REE and increase in Ca and Si during the alteration of Y, REE, Nb, Ta, Ti-oxide minerals were recorded by several authors (e.g. Nasraoui and Bilal 2000; Ercit 2005; Geisler et al. 2005; Ruschel et al. 2010).

6. Conclusions

“Písekite” aggregate, a fine-grained mixture of mostly metamict U, Th-enriched Y, REE, Nb, Ta, Ti-oxide minerals (primary precursors – polycrase-(Y) ~ samarskite-

(Y) > fergusonite-(Y)) from Obrázek I pegmatite, Písek, underwent a low-temperature hydrothermal alteration at <150–200 °C. The secondary assemblages are dominated by Fe-rich smectite and include also pharmacosiderite and kahlerite/metakahlerite. The altered REE zones of “písekite” aggregate are depleted in Y and $REE > U$ and significantly enriched in Si, As and P. The newly-formed products include U, Nb, Ti, Fe, As, P-rich phases of variable chemical composition: phase A (Nb > Ti > Fe > U > As), phase B (U ~ Nb > Ti > As > P > Fe) and phase C (U > Nb > As > Fe > Ti). The textural features show that replacement of the Fe-rich smectite by the U, Nb-rich phases took place on a micrometer scale. The highly heterogeneous U, Nb-rich phases likely represent a mixture of nanoscale hydrated oxides, phosphates–arsenates as well as silicates of U, Fe and Ca.

Acknowledgements. The authors thank to the reviewers A. Deditius and P. Uher, and the Guest Editor J. Plášil for the constructive reviews, which significantly improved the original manuscript. This work was supported by the project of Grant Agency of Academy of Czech Republic no. KJB 301630801 to RŠ and the research project MSM0021622412 (INCHEMBIOL) to MN.

References

- BOUŠKA V, JOHAN Z (1972) New data on písekite. *Lithos* 5: 93–103
- BREITER K, CEMPÍREK J, KADLEC T, NOVÁK M, ŠKODA R (2010) Granitic pegmatites and mineralogical museums in Czech Republic. *Acta Mineral Petrogr, Field Guide Series* 6: 1–56
- ČECH F (1985) Mineralogy of Granitic Pegmatites of the Czech Part of the Bohemian Massif. Unpublished dissertation, Charles University, Prague, pp 1–333 (in Czech)
- ČERNÝ P, ERCIT T S (2005) The classification of granitic pegmatites revisited. *Canad Mineral* 43: 2005–2026
- ČERNÝ P, NOVÁK M, CHAPMAN R, FERREIRA KJ (2007) Subsolidus behavior of niobian rutile from the Písek region, Czech Republic: a model for exsolution in W- and Fe²⁺>>Fe³⁺-rich phases. *J Geosci* 52: 143–159
- DEKOV VM, CAUDROS J, SHANKS WC, KOSKI RA (2008) Deposition of talc–kerolite–smectite–smectite at seafloor hydrothermal vent fields: evidence from mineralogical, geochemical and oxygen isotope studies. *Chem Geol* 247: 171–194
- DRAHOTA P, FILIPPI M (2009) Secondary arsenic minerals in the environment: a review. *Environ Internat* 35: 1243–1255
- ERCIT TS (2005) Identification and alteration trends of granitic-pegmatite-hosted (Y,REE,U,Th)–(Nb,Ta,Ti) oxide minerals: a statistical approach. *Canad Mineral* 43: 1291–1303
- EWING RC (1975) Alteration of metamict, rare-earth, AB₂O₆-type Nb–Ta–Ti oxides. *Geochim Cosmochim Acta* 39: 521–530
- GEISLER T, SEYDOUX-GUILLAUME AM, PÖML P, GOLLASCHINDLER U, BERNDT JR, WIRTH R, POLLOK K, JANSSEN A, PUTNIS A (2005) Experimental hydrothermal alteration of crystalline and radiation-damaged pyrochlore. *J Nuclear Mater* 344: 17–23
- KREJČÍ A (1923) Písekite, a new radioactive mineral or pseudomorph. *Čas Mineral Geol* 1: 1–5
- LONDON D, ČERNÝ P, LOOMIS JL, PAN JJ (1990) Phosphorus in alkali feldspars of rare-element granitic pegmatites. *Canad Mineral* 28: 771–786
- MORTON A, HALLSWORTH CR (1999) Processes controlling the composition of heavy mineral assemblages in sandstones. *Sed Geol* 124: 3–29
- NASRAOUI M, BILAL E (2000) Pyrochlores from the Lueshe carbonatite complex (Democratic Republic of Congo): a geochemical record of different alteration stages. *J Asian Earth Sci* 18: 237–251
- NOVÁK M, ČERNÝ P, KIMBROUGH DL, TAYLOR MC, ERCIT TS (1998) U–Pb ages of monazite from granitic pegmatites in the Moldanubian Zone and their geological implications. *Acta Univ Carol, Geol* 42: 309–310
- NOVÁK M, JOHAN Z, ŠKODA R., ČERNÝ P, ŠREIN V, VESELOVSKÝ F (2008) Primary oxide minerals in the system WO₃–Nb₂O₅–TiO₂–Fe₂O₃–FeO and their breakdown products from the pegmatite No. 3 at Dolní Bory-Hatě, Czech Republic. *Eur J Mineral* 20: 487–499
- PÖML P, MENNEKEN M, STEPHAN T, NIEDERMEIER DDR, GEISLER T, PUTNIS A (2007) Mechanism of hydrothermal alteration of natural self-irradiated and synthetic crystalline titanate-based pyrochlore. *Geochim Cosmochim Acta* 71: 3311–3322
- POUCHOU, JL, PICOIR, F, (1985) “PAP” (ppZ) procedure for improved quantitative microanalysis. In: ARMSTRONG JT (ed) *Microbeam Analysis*. San Francisco Press, pp 104–106
- POVONDRA P (1981) The crystal chemistry of tourmalines of the schorl–dravite series. *Acta Univ Carol Geol* 1981: 223–264
- RUSCHEL K, NASDALA L, RHEDE D, WIRTH R, LENGAUER CH, LIBOWITZKY E (2010) Chemical alteration patterns in metamict fergusonite. *Eur J Mineral* 22: 425–433
- SEJKORA J, LITOCHEB J, EXNAR P, ČERNÝ P, ČECH F (1998) Some physico-chemical data for pink beryl (morganite) from the Písek pegmatites. *Věst Čes Geol Úst* 73: 347–350 (in Czech with English summary)
- ŠKODA R, NOVÁK M, GADAS P, ČÍCHA J, HEROLDOVÁ N (2010) Hydrothermal alteration of Y, REE, Nb, Ta, Ti-oxide minerals from the Písek pegmatites, Czech Republic: a low-temperature As enrichment. *Acta Mineral Petrogr, Abstract Series* 6: 475